Conductivity Study of Polyaniline-Cobalt Ferrite (PANI-CoFe$_2$O$_4$) Nanocomposite

E. E. Tanrıverdi[1], A. T. Uzumcu[2], H. Kavas[3], A. Demir[1], A. Baykal[1,*]

Abstract: In this investigation, the structural and electrical properties of nanocomposites of polyaniline (PANI) and cobalt ferrite synthesized by hydrothermal route are reported for the first time (with weight ratios of CoFe$_2$O$_4$/PANI 1:2 and 2:1). Synthesized nanomaterials have been characterized by XRD, FT-IR, SEM and TEM techniques. FT-IR results confirm the presence of CoFe$_2$O$_4$ and PANI in the samples. Their detailed conductivity measurements have been investigated. It has been found that PANI has a more effective conducting mechanism in CoFe$_2$O$_4$-PANI composites. These results are also consistent with the change in AC conductivity orders in composites.

Keywords: CoFe$_2$O$_4$/PANI; Hydrothermal; Nanomaterials; Permittivity; Magnetism

Introduction

Polyaniline (PANI) is a conducting polymer studied extensively due to its ease of preparation, good processibility, environmental stability and potential applications in the catalysis, biosensors, batteries, and electronic technology [1]. It can also be applied as a corrosion resistant and light-weight material [2]. The PANI composites containing nanoparticles are usually investigated due to their unique magnetic and electrical characteristics. Metal oxides with the spinel structure constitute an important class of materials exhibiting a wide variety of interesting electrical, magnetic, and optical properties [3]. Spinel ferrites which have a general structure of $[M^{2+}]_{tet}[Fe^{3+}]_{octa}O_4$ [4] exhibit noteworthy magnetic, electrical, and catalytic characteristics among magnetic materials [5,6]. When their particle size is in the nanometer range, the properties of spinel ferrites are improved remarkably [2]. Cobalt ferrite (CoFe$_2$O$_4$) belongs to the family of spinel-type ferrites and is one of the most technologically important ferrites for high-density magneto-optic recording applications, due to its high coercivity, moderate magnetization, very high magnetocrystalline anisotropy, chemical stability and mechanical hardness [7-11]. Cobalt ferrite can also be an alternative ceramic material for the development of novel magnetostrictive smart materials [12,13]. Recent studies on CoFe$_2$O$_4$ have demonstrated that it can be an appropriate material for the development of new technologies in the areas of strategic importance [10,14]. For example, CoFe$_2$O$_4$ acts as a thin absorber working at a high frequency band [15]. In addition, cobalt ferrite containing composites have been shown to exhibit an enhanced magneto-optical effect and a large magneto-electric effect [16,17]. Indeed, many recent publications have appeared in the literature on conducting and magnetic polyaniline composites containing nanoparticles such as Fe$_3$O$_4$ [18], Mn$_3$O$_4$ [19], ZnO [1], ZnFe$_2$O$_4$ [2] and NiFe$_2$O$_4$ [20].

Although many articles on the nanocomposites of

[1]Department of Chemistry, Fatih University, B. Cekmece, 34500 Istanbul, Turkey
[2]Department of Polymer Engineering, Yalova University, 77100 Yalova, Turkey
[3]Department of Physics, Gebze Institute of Technology, 41400 Cayirova, Izmit, Turkey
*Corresponding author. E-mail: hbaykal@fatih.edu.tr. Tel:+90 212 8663300; Fax: +90 212 8663402

PANI with magnetic nanoparticles have been published recently [2,19], there are very few studies on PANI-$CoFe_2O_4$ [21]. The dielectric properties and losses of a material are important since it is usually not possible to infer the connectivity of a composite system from transmission electron microscopy (TEM) and scanning electron microscopy (SEM) alone [22]. However, to the best of our knowledge, no study has been reported on dielectric behavior of PANI-$CoFe_2O_4$. In this study, synthesis, characterization and electrical properties of $CoFe_2O_4$-PANI nanocomposites have been investigated for the first time.

Experimental

Chemicals

Cobalt chloride ($CoCl_2 \cdot 6H_2O$), iron chloride ($FeCl_3 \cdot 6H_2O$), and NaOH were purchased from Merck; $(NH_4)_2S_2O_8$ (APS, as initiator) and cetyl trimethyl ammonium bromide (CTAB) were obtained from Sigma-Aldrich and were used as received without further purification. Aniline monomer, obtained from Sigma-Aldrich, was distilled twice under reduced pressure before use.

Instrument

X-ray powder diffraction (XRD) analysis was conducted on a Rigaku Smart Lab Diffractometer operated at 40 kV and 35 mA using Cu K_α radiation. Fourier transformed infrared (FT-IR) spectra were measured in transmission mode with a Perkin Elmer BX FT-IR infrared spectrometer. The powder samples were grounded with KBr and compressed into pellets. FT-IR spectra in the range 400~4000 cm^{-1} were recorded in order to investigate the nature of the chemical bonds formed. The real (ε') and imaginary (ε'') parts of complex dielectric permittivity $\varepsilon^* [= \varepsilon'(\omega) + i\varepsilon''(\omega)]$ were measured with a Novocontrol dielectric-impedance analyzer. The dielectric data ($\varepsilon', \varepsilon''$) were collected during heating as a function of frequency. The films were sandwiched between gold blocking electrodes and the conductivities were measured in the frequency range 0.1 Hz

to 3 MHz at 283 K intervals. The temperature was controlled with a Novocontrol cryosystem, which is applicable between 293 and 393 K. Static magnetic properties measurements were performed using a quantum design vibrating sample magnetometer (QD-VSM). SEM analysis was performed on FEI XL40 Sirion FEG digital scanning microscope, and samples were coated with gold at 10 mA for 2 min prior to analysis. TEM analysis was carried on a FEI Tecnai G2 Sphera microscope, with TEM sample preparation of having a drop of diluted sample in alcohol dripping onto a grid.

Procedure

Synthesis of $CoFe_2O_4$ Nanoparticles

In a typical experiment, stoichiometric amount of cobalt chlorides and iron (III) chloride (with 1:2 molar ratio) were completely dissolved in 20 ml distilled water under stirring. Then certain amount of NaOH was added until the pH value of the solution reached 11. After continuous stirring for an hour, a homogeneous solution can be obtained. The mixed solution was poured in to a Teflon lined stainless-steel autoclave (60 ml) with a filling degree of 60%. The autoclave was kept at 423 K for 12 h, and then cooled to room temperature naturally. The product was filtered and washed several times with distilled water and absolute ethanol, and then dried in a vacuum oven at 343 K for 6 h.

Synthesis of $CoFe_2O_4$-PANI

Detailed synthesis of PANI was reported in our previous study [19]. Briefly, 1 g of aniline was dissolved in a dispersion of 0.1 g Mn_3O_4 nanoparticles and 0.2 g CTAB in 50 ml water at room temperature. The polymerization was carried out at 273-278 K for 8 h after the drop-wise addition of 20 ml of 0.1 M HCl/precooled APS solution into the mixture with constant stirring. The product was isolated by washing the reaction mixture with deionized water and ethanol, followed by drying under vacuum at 323 K for 4 h. The synthesis of $CoFe_2O_4$-PANI mixture was carried out in accordance to the description in the table listed in the Section of Figures and Table 1.

Table 1   Experimental conditions

Sample	Code	$CoFe_2O_4$ (gm)	PANI (gm)	$CoFe_2O_4$/PANI (w/w)
$CoFe_2O_4$	1A	0.2	–	–
$CoFe_2O_4$/PANI	1A1	0.2	0.1	2:1
$CoFe_2O_4$/PANI	1A2	0.2	0.4	1:2
PANI	–	–	0.2	–

Results and Discussion

XRD Analysis

The XRD patterns of the prepared $CoFe_2O_4$ (1A) (Fig. 1(a)) show six reflection planes: (220), (311), (400), (422), (511) and (440), which indicates the presence of the spinel cubic structure [23] and agrees with that reported in JCPDS Card No. 22-1086. The average crystallite diameter (L) was estimated by Scherrer's equation, $L=0.9\lambda/\beta\cos\theta_B$ (where β is the line broadening at the full-width at half maximum (FWHM) of the most intense peak (311), θ is the Bragg angle, and λ is the X-ray wavelength) [24,25]. The result shows that the particle size of $CoFe_2O_4$ was calculated as 5 ± 3 nm. By the addition of the PANI, the crystallinity decreases for 1A1 and 1A2 samples (Fig. 1(b) and 1(c)). An almost amorphous structure of PANI was observed in Fig. 1(d).
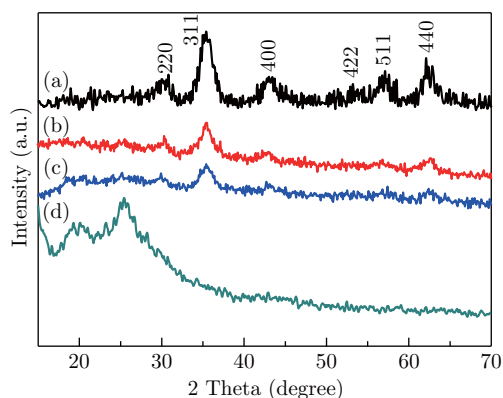

Fig. 1 XRD powder patterns of (a) 1A; (b) 1A1; (c) 1A2; and (d) PANI.

FT-IR Analysis

Figure 2(a)-2(d) shows the FT-IR spectra of the $CoFe_2O_4$ nanoparticles, PANI-$CoFe_2O_4$ composite (1A1 and 1A2) and pure PANI, respectively. Two absorption bands are observed at 566 and 493 cm^{-1}, which can be attributed to the coupling between Fe-O stretching modes of tetrahedral and octahedral sites as expected from normal spinel structure [26,27]. Figure 2(b) and 2(c) shows the IR spectra of PANI and PANI-$CoFe_2O_4$ mixtures. The peaks at 1564 and 1488 cm^{-1} are attributed to the characteristic C=C stretching of the quinoid and benzenoid rings, and 1303 and 1246 cm^{-1} are assigned to C-N stretching of the benzenoid ring. The broad peak at 1143 cm^{-1}, which is described by Quillard et al. as the "electronic-like band" [28], is associated with the vibration mode of N=Q=N (Q refers to the quinonic-type rings). The peak at

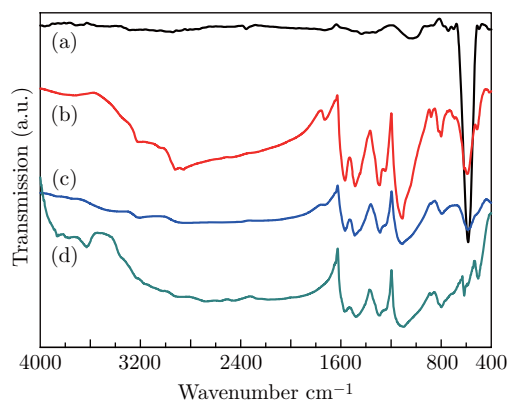804 cm^{-1} is attributed to the out-of-plane deformation of C-H in the p-disubstituted benzene ring [19].

Fig. 2 FT-IR spectra of: (a) 1A; (b) 1A1; (c) 1A2; and (d) PANI.

TEM & SEM Analysis

A typical TEM micrograph was shown in Fig. 3(a) for $CoFe_2O_4$ nanoparticles. SEM micrographs of PANI-$CoFe_2O_4$ with different amount of PANI were shown in Fig. 3(b). The nanoparticles for both materials consist of spherical particles. For $CoFe_2O_4$ nanoparticles, the average particle size observed by TEM measurements was found to be 6.8 ± 0.1 nm. This value is in good agreement with the value estimated from the XRD data. $CoFe_2O_4$ nanoparticles (1A) were found to be embedded in PANI as shown in Fig. 3(b).

Conductivity

AC Conductivity

The AC conductivity characteristic of 1A, 1A1 and 1A2 composites and pure PANI samples are measured between 293 and 373 K in 1Hz-3MHz frequency range (Fig. 4). All measurements are carried out from 293 to 373 K. The AC conductivity of 1A increases with increasing frequency exponentially and has same values for high frequencies at all elevated temperatures. Total conductivity σ_T of ferrites (1A), PANI and their composites (1A1 and 1A2) can be analyzed with the equation of $\sigma_T=\sigma_{DC}(T) + \sigma(\omega)$ [29], which is due to their semiconducting nature at elevated temperatures and frequencies. The first term in this equation is σ_{DC} which is related to the drift of electric charge carriers via band conduction mechanism and its temperature dependence relationship can be elevated by following Arrhenius relation: $\sigma_{DC}=\sigma_0 + \exp(-E_a/kT)$. The second term $\sigma(\omega)$ depends on frequency which related to the dielectric relaxation caused by the localized electric charge carriers. It obeys the empirical formula of
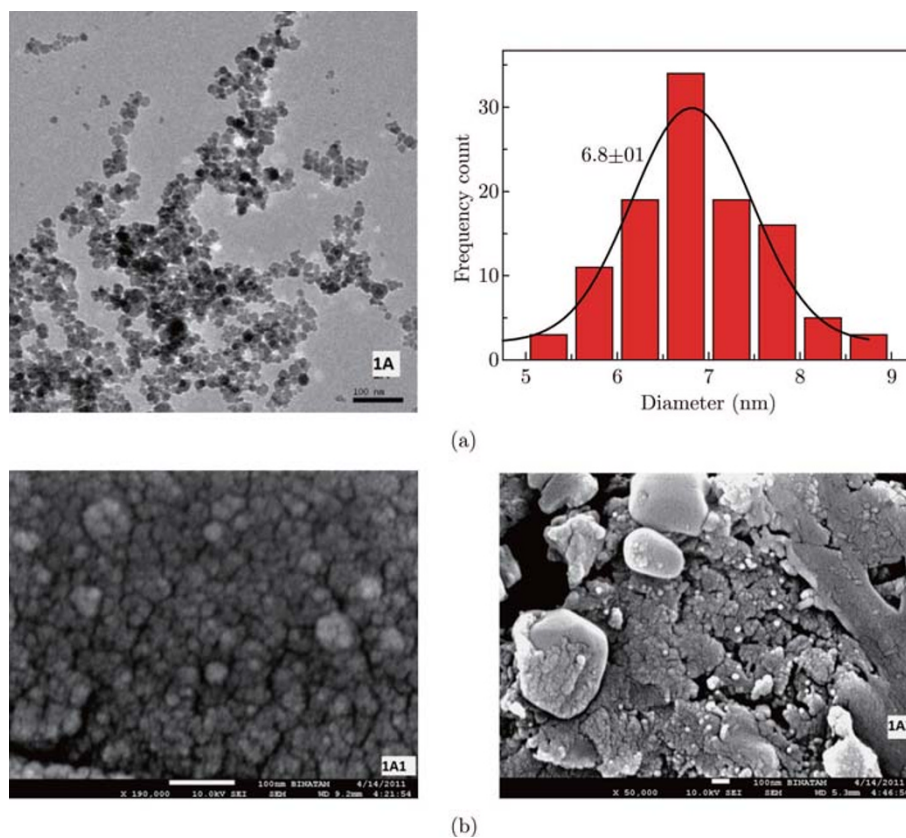
Fig. 3   (a) TEM micrograph with log normal distribution of 1A; and (b) SEM pictures of 1A1 and 1A2.
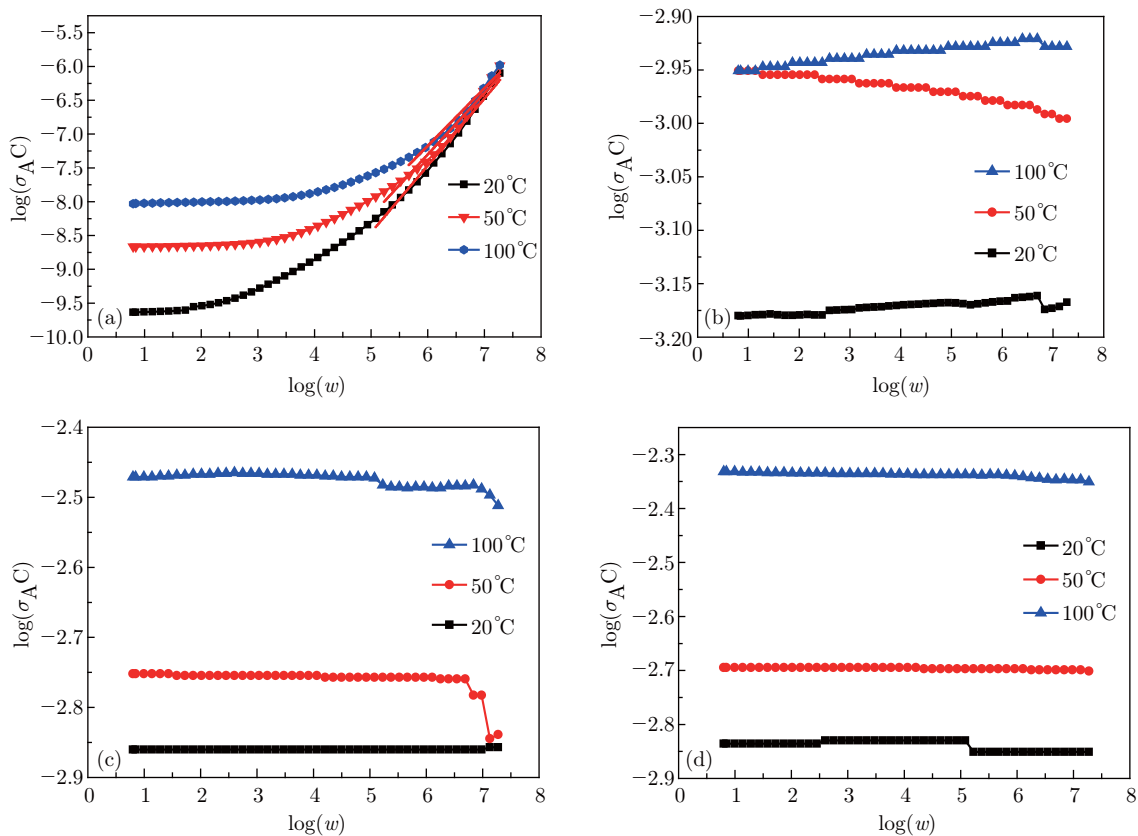

Fig. 4   AC conductivity vs. frequency for all samples: (a) 1A; (b) 1A1; (c) 1A2; (d) PANI.

frequency dependence given by AC power law [30],

$$\sigma = B(T)w^{n(T)} \tag{1}$$

in which $B(T)$ and $n(T) \leq 1$ are constants at a certain temperature. The logarithm of AC conductivity versus angular frequency curves for 1A were fitted according to Eq. 1, and the fitting curves are shown as continuous lines in Fig. 4(a). The temperature dependence of fitting parameters of n is shown in Fig. 5. The cobalt ferrite nanoparticles (1A) have a conduction mechanism of Overlap Large Polarons (OLP), which is inferred from the variation of n with respect to temperature. In OLP conduction mechanism, n shows a decrease initially. After reaching a minimum it starts to increase again with temperature [30].
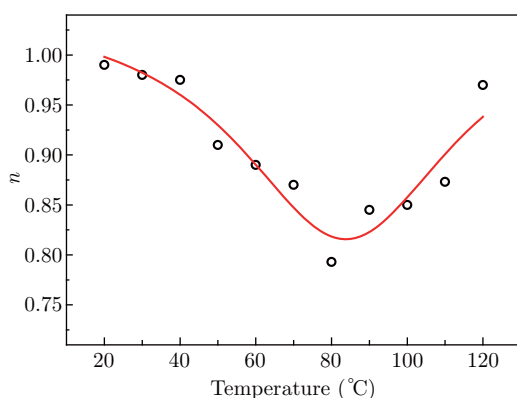

Fig. 5   Variation of fitting parameter of n with respect to temperature for 1A.

The AC conductivity curve of pure PANI has three different regimes at 293 K. At higher temperatures it can be seen that the variation of conductivity by increasing frequency exists three regimes: it increases in Regime I, almost unchangeable in Regime II, and decreases in Regime III (see Fig. 4(d)). This behavior is in agreement with the evidence of Fig. 7 in ref [31]. The conductivity mechanism may be explained by dielectric properties in the next section. The conductivities of double- or half-weight cobalt ferrite composite (1A1 and 1A2) have almost the same order of magnitude comparing with that of PANI. Therefore the addition of cobalt ferrite into PANI does not have a significant effect at 293 K; but the trend of conductivity curves can vary at higher temperatures. PANI is more effective in conduction than $CoFe_2O_4$ (1A), that is, the ratio of PANI to $CoFe_2O_4$ in the composite is 1:2 (1A2).

DC Conductivity

The DC conductivity values derived from the extrapolation of AC conductivity curves at lower frequencies are shown in Fig. 6. The activation energies are obtained from the slope of the Arrhenius curves by using the following equation [32],

$$\tilde{\sigma} = \sigma_o + \exp(E_\sigma/kT). \tag{2}$$

in which σ is a temperature-dependent term and E_A is the activation energy. The fitting curves in continuous lines are shown in Fig. 6. The obtained activation energies are as follows: 3.85 meV, 0.44 meV, 1.33 meV and 1.42 meV for 1A, 1A1, 1A2 and pure PANI, respectively.
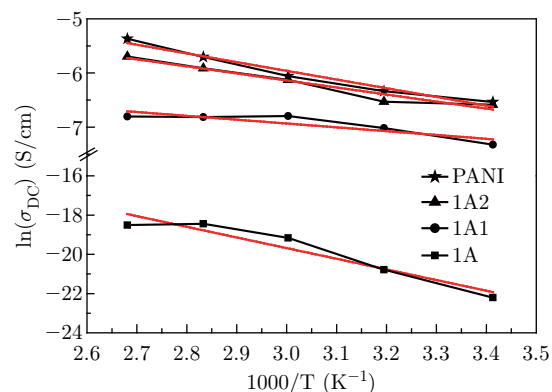

Fig. 6   Arrhenius plot of DC conductivity and 1000/T with their fits.

At room temperature the DC conductivity of composites 1A1 and 1A2, as well as pure samples 1A and PANI are significantly increased with increase of PANI weight percentage (see Fig. 7). This indicates that PANI has a more effective conducting mechanism in $CoFe_2O_4$-PANI composites (1A1 and 1A2). This result is also consistent with the change in the order of AC conductivity in composites. According to the ref [31], the AC conductivity curves of PANI-DBSA/PVF composites would jump if the composite contains more than 20% weight of PANI. In another study, the critical filling ratio for PANI is found to be around 20% for Ce_2O-PANI composites [33].
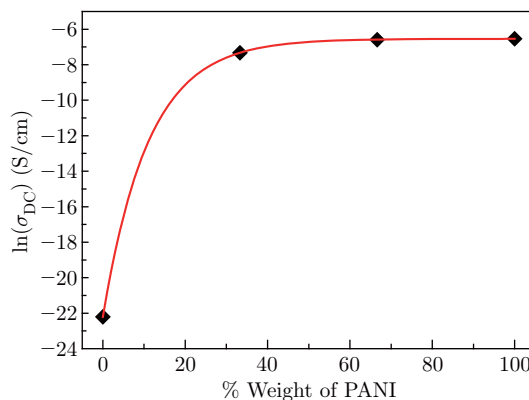

Fig. 7   DC conductivity vs weight percantage of PANI.

Permittivity

The permittivity of the samples are shown in Fig. 8. At lower frequencies both ε' and ε'' of $CoFe_2O_4$ (1A) initially decrease exponentially, and then increase with rising temperature. However, they all have the same characteristics at higher frequencies. For all samples the ε'' curves exhibit a sharp decrease at lower frequency, whereas, they become stable at higher fre-

quency and also show independent trends on temperature (Fig. 8(e)-8(h)). However the ε' values of PANI are negative, whereas, they are positive for $CoFe_2O_4$. The composites 1A2 predominated by PANI have negative ε' values, and 1A1 predominated by $CoFe_2O_4$ have positive values initially, and then fluctuate at negative values, and finally become steady above 100 Hz (see Fig. 8(a)-8(d)).
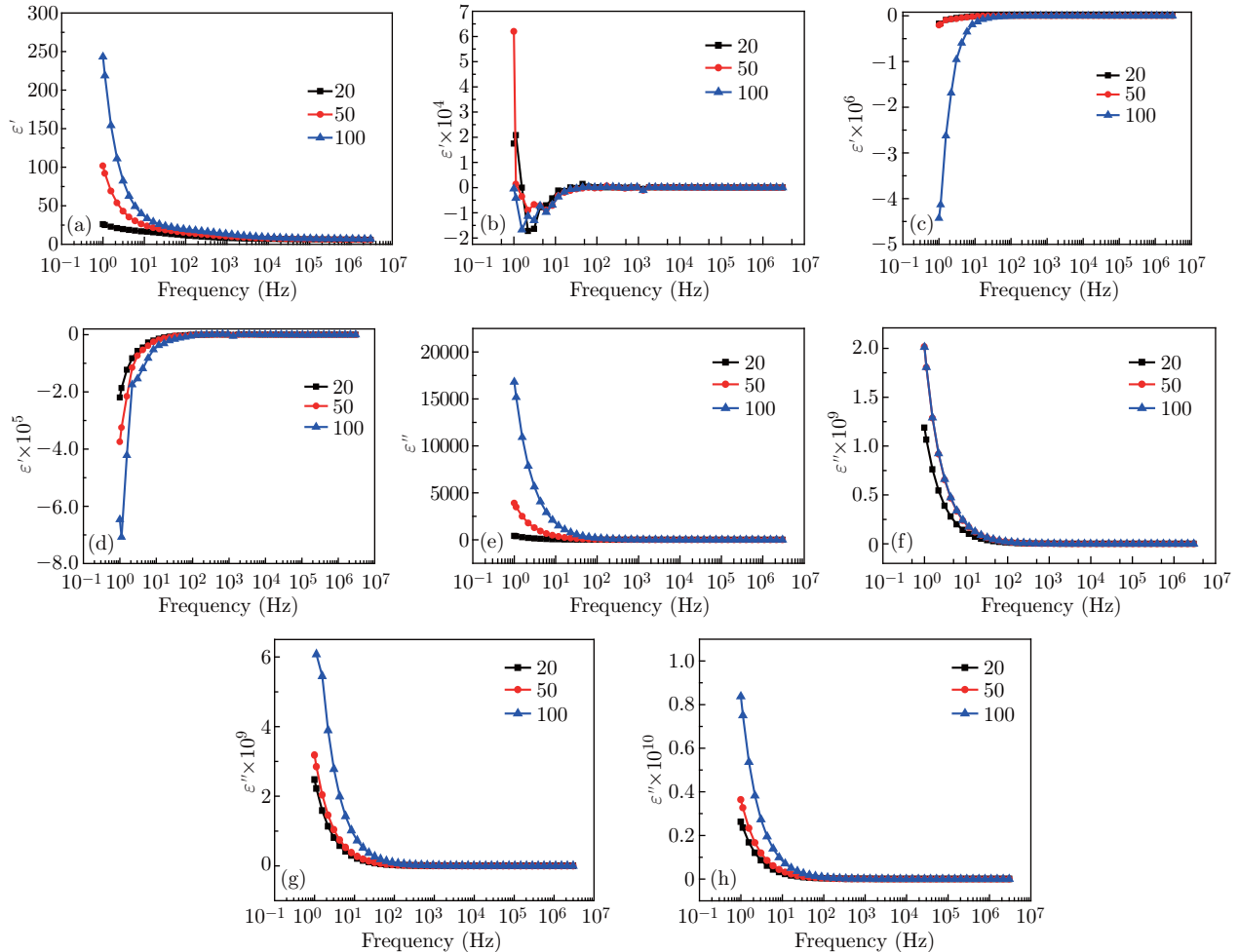

Fig. 8   Real part of permittivity for: (a) 1A; (b) 1A1; (c) 1A2; and (d) PANI. Imaginary part of permittivity for: (e) Cobalt Ferrite; (f) 1A1; (g) 1A2; and (h) PANI.

The primarily negative permittivity may be attributed to the large plasmon resonance conductivity at relatively low frequency [34]. The unique negative permittivity observed at low frequency for PANI samples implicate their potential applications in high temperature superconductors [35].

There are several theories to explain the mechanism on how the dielectric properties of the composite depend on mixing polymer and host material dielectric properties [36]. The first one is the volume fraction average method which was applied to determine the ef-

fective dielectric constant,

$$\varepsilon_{eff} = \phi_1\varepsilon_1 + \phi_2\varepsilon_2 \tag{3}$$

where ϕ is the volume fraction of the constituents.

The second equation is Maxwell equation, and the effective parameter is represented by

$$\varepsilon_{eff} = \varepsilon_1 \frac{\varepsilon_2 + 2\varepsilon_1 - 2(1-\phi_1)(\varepsilon_1 - \varepsilon_2)}{\varepsilon_2 + 2\varepsilon_1 + 2(1-\phi_1)(\varepsilon_1 - \varepsilon_2)} \tag{4}$$

It is based on a mean field approximation of a single spherical inclusion surrounded by a continuous matrix

of the polymer [37]. The room temperature dielectric constants ε' and ε' of constituents and composites are shown in Fig. 9 and Fig. 10, respectively. As a result, the volume fraction model can be more realistic to determine the dielectric properties of our composites. Although it is implied in the literature that the Maxwell equation is more realistic than volume fraction model

[36], the latter has been found to be more accurate. Because of the large order of difference between the dielectric constants of constituents (ε' for $CoFe_2O_4$ is 25, and for PANI is -2×10^5, almost 10^4-fold difference in dielectric properties of constituents may be explained by dominant dielectric properties of PANI/$CoFe_2O_4$.
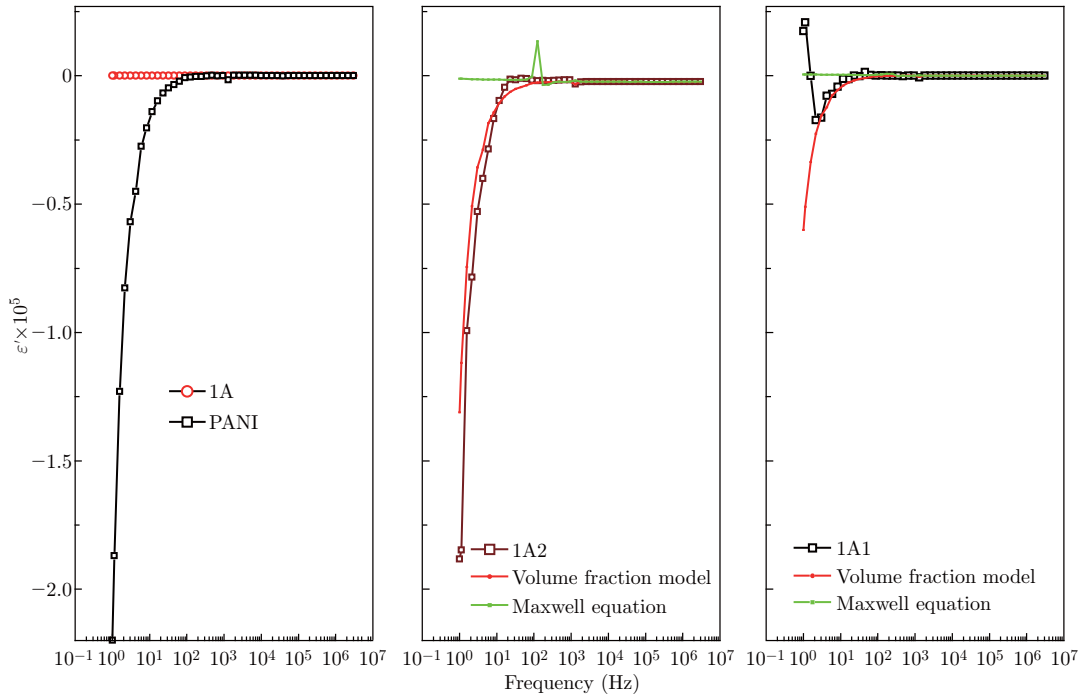

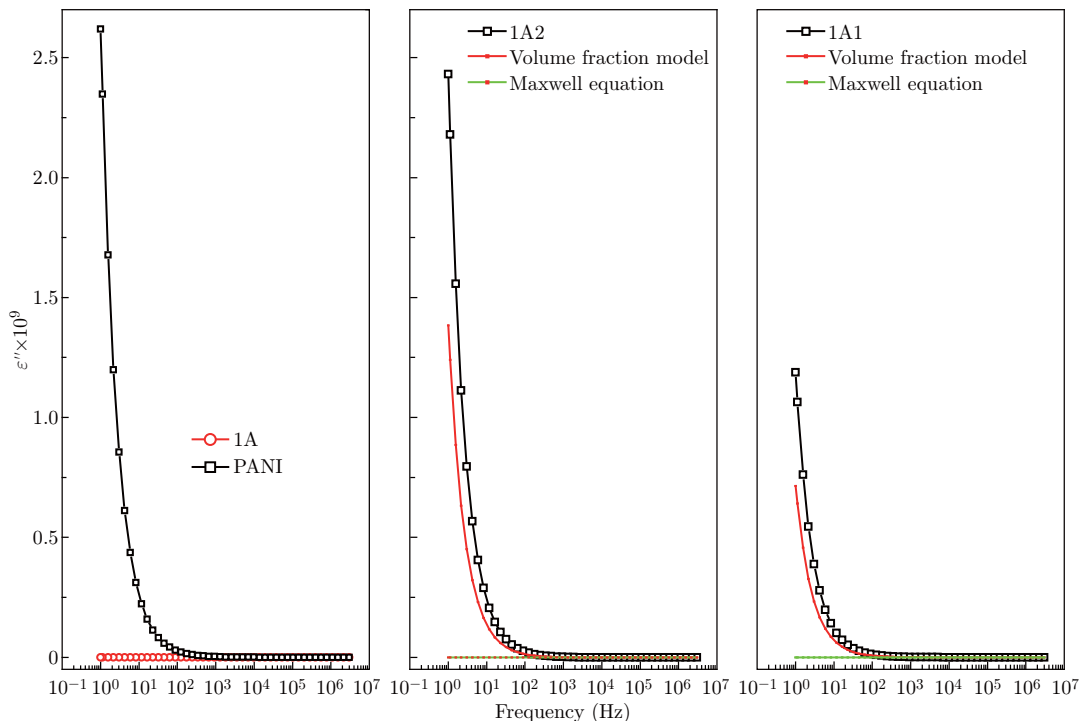Fig. 9 Room temperature dielectric constants (ε') of 1A, 1A1, 1A2 and PANI.

Fig. 10 Room temperature dielectric constants (ε'') of 1A, 1A1, 1A2 and PANI.

Conclusion

In this study, the synthesis, conductivity and permittivity characterization of the composite of $CoFe_2O_4$-PANI (with the weight ratio of 1:2 and 2:1) have been reported. The XRD study reveals the formation of cubic spinel structure; and all of the characteristic reflection peaks have a (311) reflection trend. It has also been found that volume fraction model shows more accurate results compared with the Maxwell equation.

Acknowledgment

References

[1] S. Ameen, M. S. Akhtar, S. G. Ansari, O. B. Yang and H. S. Shin, Superlattices Microst. 46, 872 (2009). http://dx.doi.org/10.1016/j.spmi.2009.09.007

[2] G. D. Prasanna, H. S. Jayanna and V. Prasad, J. Appl. Polym. Sci. 120, 2856 (2011). http://dx.doi.org/10.1002/app.33304

[3] M. J. Iqbal and B. Ismail, Journal of Alloys and Compounds 472, 434 (2009). http://dx.doi.org/10.1016/j.jallcom.2008.04.079

[4] P. Siwach, S. Singh and R. K. Gupta. Catal. Commun. 10, 1577 (2009). http://dx.doi.org/10.1016/j.catcom.2009.04.019

[5] A. R. Shyam, R. Dwivedi, V. S. Reddy, K. V. R. Chary and R. Prasad, Green Chem. 4, 558 (2002). http://dx.doi.org/10.1039/b207410a

[6] S. V. Reddy, S. A. Radhe, R. Dwivedi, R. K. Gupta, V. R. Chumbale and R. Prasad, J Chem. Technol. Biotechnol. 79, 1057 (2004). http://dx.doi.org/10.1002/jctb.1060

[7] S. D. Bhame and P. A. Joy, J. Phys. D: Appl. Phys. 40, 3263 (2007). http://dx.doi.org/10.1088/0022-3727/40/11/001

[8] S. A. Chambers, R. F. C. Farrow, S. Maat, M. F. Toney, L. Folks, J. G. Catalano, T. P. Trainor and G. E. Brown Jr., J. Magn. Magn. Mater. 246, 124 (2002). http://dx.doi.org/10.1016/S0304-8853(02)00039-2

[9] J. G. Do S. Duque, M. A. Macedo and N. O. Moreno, Phys. Stat. Sol. 220, 413 (2000).

[10] M. S. Khandekar, R. C. Kambale, J. Y. Patil, Y. D. Kolekar and S. S. Suryavanshi, J. Alloys Compd. 509, 1861 (2011). http://dx.doi.org/10.1016/j.jallcom.2010.10.073

[11] M. C. Terzzoli, S. Duhalde, S. Jacobo, L. Steren and C. Moina, J. Alloys Compd. 369, 209 (2004). http://dx.doi.org/10.1016/j.jallcom.2003.09.086

[12] R. C. Kambale, P. A. Shaikh, N. S. Harale, V. A. Bilur, Y. D. Kolekar, C. H. Bhosale and K. Y. Rajpure, J. Alloys Compd. 490, 568 (2010). http://dx.doi.org/10.1016/j.jallcom.2009.10.082

[13] R. W. McCallum, K. W. Dennis, D. C. Jiles, J. E. Snyder and Y. H. Chen, Low Temp. Phys. 27, 266 (2001). http://dx.doi.org/10.1063/1.1365598

[14] M. A. Ahmed, N. Okasha, S. F. Mansour and S. I. El-dek, J. Alloy. Compd. 496, 345 (2010).

[15] J. Cao, W. Fu, H. Yang, Q. Yu, Y. Zhang, S. Liu, P. Sun, X. Zhou, Y. Leng, S. Wang, B. Liu and G. Zou, J. Phys. Chem. B 113, 4642 (2009). http://dx.doi.org/10.1021/jp8093287

[16] F. Cheng, C. Liao, J. Kuang, Z. Xu, C. Yan, L. Chen, H. Zhao and Z. Liu, J. Appl. Phys. 85, 2782 (1999). http://dx.doi.org/10.1063/1.369594

[17] J. Ryu, S. Priya, K. Uchino and H. Kim, J. Electroceram. 8, 107 (2002). http://dx.doi.org/10.1023/A:1020599728432

[18] J. Deng, C. He, Y. Peng, J. Wang, X. Long, P. Li and A. S. C. Chan, Synth. Met. 139, 295 (2003). http://dx.doi.org/10.1016/S0379-6779(03)00166-8

[19] Z. Durmus, A. Baykal, H. Kavas and H. Sözeri, Physica B 406, 1114 (2011). http://dx.doi.org/10.1016/j.physb.2010.12.059

[20] Z. Hu, H. Zhao, C. Kong, Y. Yang, X. Shang, L. Ren and Y. Wang, J. Mater. Sci. Mater. Electron. 17, 859 (2006). http://dx.doi.org/10.1007/s10854-006-0042-z

[21] B. Su, X. Zuo, C. Hu and Z. Lei, Acta Phys. Chim. Sin. 24, 1932 (2008)-10.

[22] D. S. McLachlan and G. Sauti, J. Nanomater. 2007, Article ID 30389 (2007), http://dx.doi.org/10.1155/2007/30389

[23] A. M. El-Sayed, Ceram. Int. 28, 363 (2002). http://dx.doi.org/10.1016/S0272-8842(01)00103-1

[24] K. P. Chae, J. Lee, H. S. Kweon and Y. B. Lee, J. Magn. Magn. Mater. 283, 103 (2004). http://dx.doi.org/10.1016/j.jmmm.2004.05.010

[25] N. Gupta, A.Verma, S. C. Kashyap and D. C. Dube, J. Magn. Magn. Mater. 308, 137 (2007). http://dx.doi.org/10.1016/j.jmmm.2006.05.015

[26] A. Baykal, N. Kasapoglu, Y. Köseoglu, A. C. Basaran, H. Kavas and M. S. Toprak, Cent. Eur. J. Chem. 6, 125 (2008). http://dx.doi.org/10.2478/s11532-007-0070-4

[27] N. Kasapoğlu, A. Baykal, Y. Köseoğlu and M. S. Toprak, Scriptia Materialia 57, 441 (2007). http://dx.doi.org/10.1016/j.scriptamat.2007.04.042

[28] S. Quillard, G. Louarn, S. Lefrant and A. G. MacDiarmid, Phys. Rev. B 50, 12496 (1994). http://dx.doi.org/10.1103/PhysRevB.50.12496

[29] A. Ghosh, Phys. Rev. B 42, 1388 (1990). http://dx.doi.org/10.1103/PhysRevB.42.1388

[30] S. R. Elliott, Adv. Phys. 36, 135 (1987). http://dx.doi.org/10.1080/00018738700101971

[31] S. Ebrahim, A. Kashyout and M. Soliman, Current Applied Physics 9, 448 (2009).

[32] N. F. Mott and E. A. Davis, Electronic Processes in Non-crystalline Material, Oxford Press, London 1979.

[33] N. Parvatikar and M. V. N. Ambika Prasad, Journal of Applied Polymer Science 100, 1403 (2006). http://dx.doi.org/10.1002/app.22950

[34] F. Legros and A. Fourrier-Lamer, Mater. Res. Bull. 19, 1109 (1984). http://dx.doi.org/10.1016/0025-5408(84)90060-6

[35] C. W. Chu, F. Chen, J. Shulman, S. Tsui, Y. Y. Xue, W. Wen and P. Sheng, Proc. SPIE 5932, 59320X (2005). http://dx.doi.org/10.1117/12.626267

[36] P. Barber, S. Balasubramanian, Y. Anguchamy, S. Gong, A. Wibowo, H. Gao, H. J. Ploehn and H. Loye, Materials 2, 1697 (2009). http://dx.doi.org/10.3390/ma2041697

[37] D. Yoon, H. Zhang and J. Lee, B. I. Mater. Res. Bull. 38, 765 (2003). http://dx.doi.org/10.1016/S0025-5408(03)00075-8